JOURNAL OF Materials CHEMISTRY

Synthesis and characterisation of photonic crystals†

David W. McComb,*[a] Belinda M. Treble,[a,b] Claire J. Smith,[a] Richard M. De La Rue[b] and Nigel P. Johnson[b]

[a]*Department of Chemistry, University of Glasgow, Glasgow, UK G12 8QQ. E-mail: D.McComb@chem.gla.ac.uk*
[b]*Department of Electronic & Electrical Engineering, University of Glasgow, Glasgow, UK G12 8QQ*

Received 5th May 2000, Accepted 14th June 2000
First published as an Advance Article on the web 10th October 2000

The formation of two types of photonic crystal is described. Normal opal is formed by close packing of silica spheres. The synthesis of the silica spheres is described and some of the factors that influence the size of the spheres in the product are discussed. Three different methods for the preparation of close packed arrangements of the spheres are described and the photonic properties of the crystals produced are demonstrated. Inverse opal is based on a close packed array of "air" spheres in a dielectric matrix. Different methods for the formation of this ordered microporous solid based on titanium dioxide are described and the photonic properties of this material are discussed.

1 Introduction

Dielectric crystal-like lattices, termed photonic crystals, have been the subject of numerous investigations since the original work by Yablonovitch[1] and John.[2] The concept of a photonic crystal is appealingly simple; periodic electromagnetic modulation created by a lattice of dielectric "atoms" can yield a gap of forbidden photon energies in a manner analogous to the way in which a periodic arrangement of atoms in a semiconductor lattice results in an electronic band gap. The potential applications of a photonic crystal exhibiting a complete photonic band gap (PBG) are considerable, ranging from high performance LEDs, through low threshold lasers to ultra compact wavelength division multiplexing (WDM) components and sources with novel photon statistical behaviour.[3] While true photonic band gap behaviour has been realised in the microwave regime using mechanically manufactured lattices, the challenge of obtaining mechanically stable three-dimensional photonic crystals that operate in the visible and near infra-red wavelength ranges is still considerable.[4]

Arguably, the first observed photonic crystal was opal, which occurs naturally in many locations in the world and has long been valued as a precious stone. Natural opal is formed in either a sedimentary or a volcanic environment and is composed of a cubic close packed (ccp) arrangement of amorphous silica spheres.[5] The spheres may range in size between 150 and 900 nm, but have a narrow size distribution (around 5%). However, the impurities present in natural opal, which colour the crystals and enhance their value, also limit their potential as photonic crystals. A full PBG requires a topologically interconnected material that exhibits a large refractive index contrast (RIC) between the "atoms" and the voids (or surrounding medium) in the lattice of the photonic crystal. In natural opal, the impurities are commonly located in the octahedral and tetrahedral interstices in the lattice and restrict the RIC that can be obtained.[5] Hence, it is desirable to form synthetic opal in clean laboratory conditions to ensure that the interstices are empty and can be used to modify the properties of the photonic crystal.

†Basis of a presentation given at Materials Discussion No. 3, 26–29 September, 2000, University of Cambridge, UK.

In silica-based opal, the achievable RIC (1.435–1.460) is below that required for realisation of a complete PBG in a crystal with conventional symmetry, although it may be sufficient in 2-D systems or in quasicrystalline arrangements.[6] The RIC can be enhanced by using spheres formed from a higher refractive index material or by filling the interstices with a second material that has a much higher refractive index.[7] The RIC of the latter can be further enhanced if the spheres can be removed from the structure to leave air-filled spherical voids.[8–12] Such a material is termed "inverse opal" and is best visualised as a close-packed array of air spheres with the interconnected octahedral and tetrahedral interstices filled with a high refractive index material.

In this paper we report some recent results on the synthesis and characterisation of opal and inverse opal photonic crystals. The first step in the formation of opal with a particular photonic stopband is the synthesis of silica spheres of a specific size and with a narrow size distribution. The results of our investigations into the factors that influence the size of the spheres produced as well as the reproducibility of the experimental procedure are discussed before describing the formation and characterisation of synthetic opal. We also report recent results on the production of inverse opal and discuss the structure–property relationship of this novel material. In order to demonstrate the photonic properties of the materials produced, the results of optical reflectance measurements on both opal and inverse opal are described.

2 Experimental procedures

The synthesis procedure for the silica spheres was a modified version of the protocol described by Stober *et al.*[13] The reagents used were tetraethyl orthosilicate (TEOS, Aldrich), ethanol (99.6%, Fisher), concentrated ammonia (Fisher) and distilled water. The TEOS and ethanol were distilled immediately before use. All of the glassware used was thoroughly cleaned and dried before use. Two mother liquors, containing TEOS–ethanol and ammonia–water–ethanol, respectively, were made up in 50 ml volumetric flasks for each experiment. The liquids were injected into the flasks using a surgical syringe fitted with a 0.2 μm filter. The ammonia concentration in the mother liquor was

 DOI: 10.1039/b003191g

This journal is © The Royal Society of Chemistry 2001

determined by back titration using 1 M HCl and 1 M NaOH. The TEOS concentration was determined by weight and the water concentration by difference. The concentrations of each component refer to their concentration in the final reaction mixture.

The mother liquors and a 250 ml reaction vessel were placed in a thermostatically controlled water bath (24.9 ± 0.1 °C) for one hour before use in order to ensure temperature equilibration. The two mother liquors were quickly combined in the reaction vessel and the mixture was agitated using a magnetic stirrer. The reaction was stoppered and left for a minimum of 16 h. Within about 5 min of mixing, the opaqueness of the solution increased noticeably. On completion, the suspension of silica spheres was filtered under suction using a 0.2 μm filter and the solid product was washed with distilled water until the pH of the filtrate was neutral. The spheres were removed from the filter paper and redispersed in ethanol for storage. The silica spheres were characterised in a JEOL 1200 transmission electron microscope (TEM). A small droplet of the spheres in ethanol was placed on a carbon-coated copper grid and the solvent was allowed to evaporate. The sample was examined in the TEM and the particle size distribution was determined from the measurements of at least 100 spheres.

For the formation of opal, an aliquot of the colloidal suspension of silica spheres in water was agitated in an ultrasonic bath to ensure complete dispersion. A polished silica substrate was placed in a thick-walled silica glass tube and about 10 ml of the colloidal dispersion was added. In the sedimentation experiments, the tube was placed in a thermostatically controlled water bath (25 °C). When sedimentation was complete, the sample was removed from the bath and any remaining water was carefully withdrawn using a pipette. The sample was dried overnight in a low temperature oven (50 °C). Two types of heat treatment were investigated as methods for improving the mechanical strength of the opal: (a) calcination of the sample at 900 °C for 24 h and (b) hydrothermal annealing in a sealed tube at 300 °C. In the centrifuge experiments, the tube was placed in an ultracentrifuge for 35 min at a speed of 3000–3500 rpm. The water was removed before the sample was dried and subsequently calcined.

The capillary experiments were based on the results published by Jiang *et al.*[14] and are closely related to the sedimentation experiments. In this method, a clean quartz substrate was positioned almost vertically in a vial containing a small amount of the colloidal dispersion. The apparatus was placed in a vibration-free, temperature-controlled environment until the majority of the liquid had evaporated, leaving a thin film of material on the quartz substrate.

The solid opal samples were examined using a scanning electron microscope (SEM, Phillips 515). In order to prevent specimen charging in the electron beam, a thin film of gold was sputtered onto the surface of the samples. The samples from the capillary experiments were also imaged in an atomic force microscope (AFM, Digital Instruments 3100 AFM/MFM) operated in contact mode. The advantage of AFM imaging is that the samples do not have to be gold-coated. Hence, the AFM can be used to identify well-ordered regions that can be subsequently investigated using optical reflectivity techniques.

3 Synthesis of silica spheres—reproducibility issues

Since the energy range of the stopbands depends directly on the size of the silica spheres used to fabricate the lattice, the aim of the current project is to develop the capability of custom synthesising spheres of any desired size. Hence, the first objective was to identify an experimental parameter that would allow the particle size of the product to be controlled. Based on the work by Stober *et al.*,[13] it was decided to investigate the effect of ammonia concentration on the particle size. The

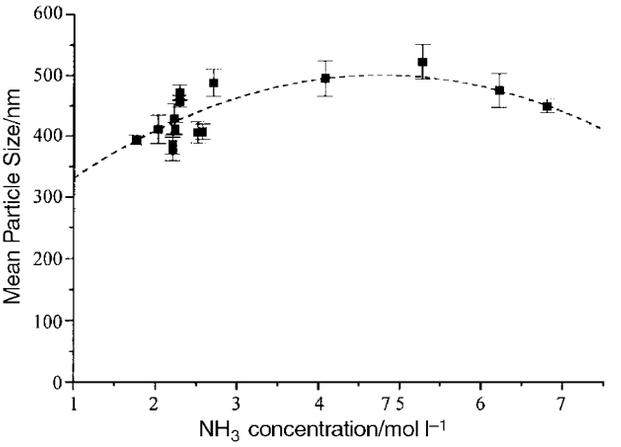

Fig. 1 Plot of the mean particle size against the concentration of ammonia in the reaction mixture. The H_2O concentration is in the range 15–16 mol l^{-1} (Table 1). The particle sizes and standard deviations (error bars) were determined from TEM measurements.

results obtained demonstrate that silica spheres in the size range 350–550 nm can be produced using ammonia concentrations in the range 1–7 mol l^{-1} (Fig. 1). The error bars shown on the figure represent the standard deviation of the particle size as measured from TEM images. It can be seen that the standard deviation is generally in the range 2–4%. In contrast with previous reports, no evidence of a systematic decrease in the standard deviation as the average particle size increases was observed.[15] The composition of the reactant mixture for each experiment is given in Table 1.

Fig. 1 and Table 1 both demonstrate that the particle size distribution is narrow and sufficiently small for the formation of good quality opal. However, it is clear that the average particle size obtained from a given reaction composition is less reproducible than is desirable, *e.g.* experiments 3 and 4 (Table 1). This effect is apparent in a number of studies reported in the literature, but the origin of the irreproducibility has not been investigated as extensively as the fundamental mechanisms of nucleation and growth.[15–18] This observation caused us some concern, as the aim of the current project has been to develop a protocol for total synthesis of opal with any desired interplanar spacing. For this reason, a number of control experiments were conducted to identify the factors that influence the reproducibility of the synthesis.

Inadequate control of the reaction temperature could potentially influence the sphere size obtained.[17] The temperature of the water bath was monitored over a period of 24 h and it was established that the absolute temperature was within ± 0.1 °C of the setpoint. Hence, it was concluded that this was unlikely to be a contributing factor.

Although the glassware was thoroughly cleaned before use it is possible that the nucleation events could be influenced by contaminants or microstructural defects on the surface of the reaction vessel. If the number of nucleation sites were varied then the average particle size would also be altered. To test this possibility, a 100 ml volume of each mother liquor was made up and each was divided into two 50 ml aliquots. The temperature equilibrated mother liquors were combined to perform two simultaneous syntheses using identical compositions. These syntheses, experiments 12a and 12b (Table 1), yielded silica spheres with essentially the same mean particle size, 571 nm and 576 nm, respectively. This synthesis was then repeated, with care taken to obtain mother liquor compositions as close to the original experiment as possible. The result, experiment 12c (Table 1), yielded silica spheres with a mean particle size of 589 nm, *i.e.* approximately 3% greater than the original result. The only difference between experiments 12c and 12a/b is the concentration of water in the reaction mixture,

Table 1 Silica sphere synthesis conditions and corresponding particle size measurements

Expt no.	Comment	[TEOS]/mol l^{-1}	[BASE]/mol l^{-1}	[H_2O]/mol l^{-1}	Average size/nm	Standard deviation (%)
1	NH_3	0.220	1.764	15.109	393	2.07
2	NH_3	0.220	2.029	15.868	411	5.69
3	NH_3	0.221	2.237	15.026	412	2.53
4	NH_3	0.221	2.293	15.064	457	2.07
5	NH_3	0.221	2.519	15.047	406	4.24
6	NH_3	0.220	2.578	16.205	407	3.06
7	NH_3	0.220	2.710	16.051	488	4.49
8	NH_3	0.220	4.080	15.062	495	5.84
9	NH_3	0.220	5.280	15.030	522	5.51
10	NH_3	0.221	6.223	15.069	475	5.89
11	NH_3	0.221	6.811	15.684	449	2.48
12a	Reproducibility	0.220	1.225	6.081	571	4.57
12b	Reproducibility	0.220	1.225	6.081	576	3.24
12c	Confirm reproducibility	0.220	1.225	6.179	589	3.76
13a	Stirring speed—fast	0.220	2.205	15.087	386	4.14
13b	Stirring speed—slow	0.220	2.205	15.087	378	5.15
14a	Addition rate—fast	0.221	2.228	15.064	428	5.76
14b	Addition rate—slow	0.221	2.228	15.064	600	13.78
15a	Addition rate—fast	0.220	2.293	14.924	472	2.65
15b	Addition rate—slow	0.220	2.293	14.924	629	4.79

which is approximately 1.6% higher in the former. However, the small difference in the particle size obtained cannot be attributed to this factor. This can be established by comparing the results from experiments 4 and 15a. In these two experiments the TEOS and ammonia concentrations are essentially identical but the concentration of water is approximately 1% higher in experiment 4. However the mean particle size obtained in experiment 4 is just over 3% smaller than in experiment 15a. On this basis it is concluded that the differences observed cannot be associated with small changes in the water concentration.

The stirring speed was one parameter that was difficult to control accurately with the experimental apparatus available. To investigate the influence of stirring speed on the sphere size of the product, simultaneous syntheses, as described above, were performed using fast and slow speeds. The results clearly demonstrate that the stirring speed has essentially no effect on the particle size of the product (experiments 13a & 13b, Table 1).

The rate of addition of one mother liquor to the other was found to have a significant effect on the particle size. This was established by conducting simultaneous experiments as described above. In experiment 14a, the mother liquors were combined as described in section 2. In experiment 14b, one of the mother liquors was added to the other at a regular rate, over a period of 3 min, using a peristaltic pump. This procedure resulted in a 40% increase in the mean particle size, but also caused a substantial increase in the standard deviation of the sphere sizes obtained (Table 1). In order to ensure that impurities which could potentially act as nucleation sites had not been inadvertently added *via* the tubing of the peristaltic pump, the experiment was repeated with new tubing that had been thoroughly cleaned. The results, experiments 15a and 15b (Table 1), show a similar increase in particle size (33%) to that previously observed but with a narrower size distribution. Therefore, it is concluded that the size distribution in experiment 14b was influenced by the presence of contaminants. However, the fact that the ratios of the standard deviations is similar in both sets of experiments suggests that the additional nucleation sites in experiment 14 may have been present in the mother liquors. Nevertheless, it is clear from the results of experiments 14 and 15 that the particle size and the size distribution of the product are dependent on the rate of addition of one mother liquor to the other.

In summary, we have produced a nearly monosized distribution of silica spheres using a modified version of the Stober–Fink–Bohn procedure. It is possible to vary the particle size of the product by varying the concentration of ammonia in the reaction mixture. The absolute value of the mean particle size differs by about 3% between repeated experiments with the same nominal composition. We have demonstrated that the mean particle size is influenced by the rate of addition of the two mother liquors. Improved experimental protocols to enable accurate control of the addition rate are currently being developed.

4 Structural characterisation of synthetic opal

Yablonovitch has reported that a cubic close packed (ccp) arrangement of silica spheres is the structure most likely to result in a complete PBG.[4] This was based on the observation that the Brillouin zone of a face centred cubic (fcc) unit cell is closest to the spherical symmetry required to ensure overlap of the PBG in all reciprocal space directions. However, other workers have suggested that the difference between ccp and hexagonal close packed (hcp) structures is rather small.[19] It is difficult to design an experimental method for packing microscopic spheres that would exclusively result in a ccp crystal. However, calculations suggest that a ccp lattice is more energetically favourable[20] and the experimental evidence tends to support this conclusion.[21,22]

In the current work, several methods to control/influence the packing of the silica spheres have been investigated. The simplest approach is to disperse the particles in a suitable liquid and allow the particles to sediment under the influence of gravity. In an attempt to improve the mechanical strength of the material produced, the sample was normally sintered at high temperature (900 °C) or, in some cases, was subjected to hydrothermal pressure. While some of the samples obtained using the sedimentation route exhibited ordered packing arrangements, the quality was variable. Although a number of researchers have obtained high quality opal using this simple approach (see, for example ref. 22), it has a number of disadvantages. The quality of the product is highly sensitive to vibration, to the evaporation rate of the liquid and to temperature fluctuations of the environment. While appropriate measures can be taken to limit these environmental factors, the main limitation is that the process is extremely slow; depending on the diameter of the spheres used, a period

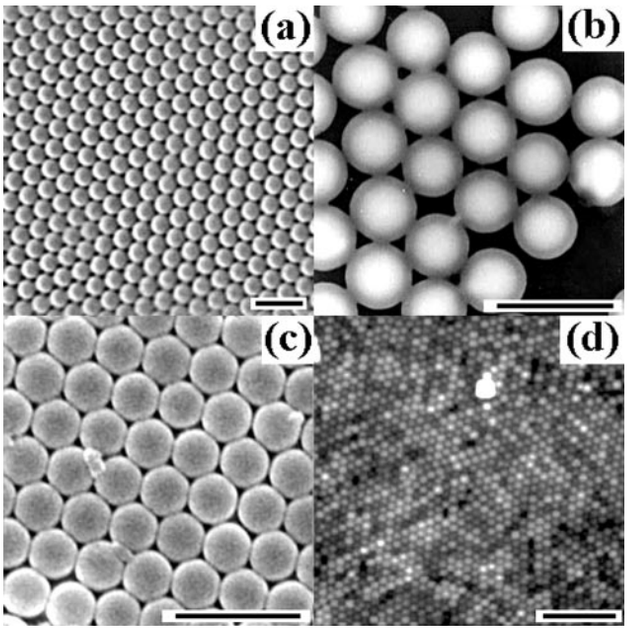

Fig. 2 (a) SEM image of opal formed using an ultracentrifuge. Scale bar = 1 μm. (b) TEM image of calcined, uncompacted silica spheres showing the formation of "necks" between the spheres. Scale bar = 1 μm. (c) High magnification SEM image of opal formed by the capillary method. Scale bar = 1 μm. (d) Large area AFM image of opal formed using the capillary method. Scale bar = 3 μm.

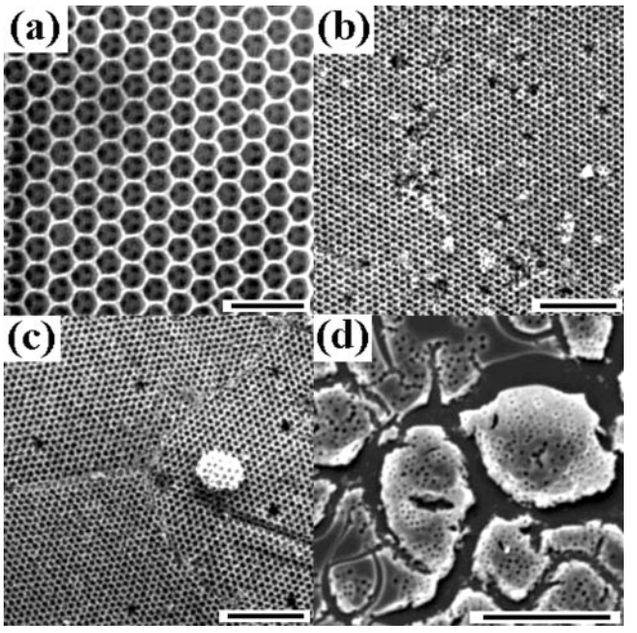

Fig. 3 (a) SEM image of inverse opal based on a close packed array of air spheres in a titania matrix. Scale bar = 1 μm. (b) SEM image showing considerable long range order in inverse opal formed using the simple filtration technique. Scale bar = 5 μm. (c) Image of the same crystal showing the presence of grain boundaries, dislocations and point defects in the crystal. Scale bar = 5 μm. (d) SEM image showing the break-up of the thin film inverse opal formed using the capillary technique. Scale bar = 5 μm.

ranging from 1 week to several months may be required to obtain a high quality sample.[22,23]

The second approach investigated was to utilise an ultracentrifuge to accelerate the packing of the spheres. Some research groups have reported that the use of a centrifuge results in disordered materials, while other groups have obtained good quality opal in this way.[24,25] The samples obtained in this project often exhibited opalescence and appeared to be well ordered when examined in the SEM (Fig. 2a). However, the drying process often resulted in crack formation and the mechanical strength of the product was poor. The hydrothermal treatment at 300 °C, described in section 2, had little effect on the mechanical strength of the product. Heat treatments at 900 °C for 24 h improve the mechanical strength of the samples and do not appear to have any detrimental effect on the ordering. It is believed that the improvement in mechanical properties is a result of the formation of "necks" between the spheres, which we have observed in control experiments on uncompacted, calcined silica powder (Fig. 2b) and has been observed by others as a result of heat treatment of opal.[26]

The objective of the "capillary" experiments described in section 2 was to develop a reliable method for the formation of thin films of opal. The specimens obtained by this method show a high degree of ordering (Fig. 2c) and opalescence is often observed. With careful control of the conditions, it is possible to obtain large areas that exhibit regular packing arrangements (Fig. 2d). In the AFM images there is significant contrast variation on a local scale, which implies height variations of the order of a sphere diameter. However, such height variations are not observed in the SEM images and appear to be an AFM artefact, possibly due to residual contamination on the surfaces of the spheres.

In summary, we have established a procedure for the rapid production of high quality opal using an ultracentrifuge. The mechanical properties of the material can be improved using appropriate heat treatments. In addition, a method for the formation of thin films of well-ordered opal has been investigated and with further refinement this method shows great promise for the production of large photonic crystals.

5 Formation and characterisation of inverse opal

We have previously reported the formation and optical properties of inverse opal based on titanium dioxide.[27] Using a combination of the approaches described by other workers,[8–11] the material was formed by infiltrating a self-organised lattice of polystyrene microspheres with titanium(IV) ethoxide, with subsequent calcination to remove the latex template and convert the organometallic precursor to TiO_2. Typically, the samples formed were 0.5 to 1 mm thick, exhibited strong opalescence and were well ordered (Fig. 3a). Electron diffraction and high resolution TEM investigations revealed that the air spheres were surrounded by a polycrystalline matrix of TiO_2 in the form of anatase.[27] However, the materials formed in this way were extremely fragile. Recently, two modified procedures have been investigated with the aim of producing high quality inverse opal with improved mechanical properties.

In the first approach a suspension of latex spheres in water was placed in a petri dish and dried overnight in a low temperature oven. This results in flakes of material approximately 1cm × 1cm in size that exhibit opalescence. These flakes were placed in a Buchner funnel located within a nitrogen glovebox to inhibit reaction of the organometallic precursor with atmospheric oxygen or water vapour. Dry ethanol, followed by titanium(IV) ethoxide was added to the funnel and then suction was applied until the white crystals were dry. At this point, no opalescence was observed. The crystals were removed from the filtration set-up and subsequently calcined in flowing air at 575 °C for 12 h. The opalescent crystals obtained in this manner are relatively robust and SEM images reveal the presence of ordered arrays of air spheres in a titania framework (Fig. 3b). While large ordered regions can be observed, the presence of grain boundaries, dislocations and vacancies shows that the crystals formed contain both extended and point defects (Fig. 3c). These structural defects could have a detrimental influence on the photonic properties of the material and methods to control the defect concentration are currently being investigated.

The second approach was to attempt capillary experiments similar to those used for the formation of normal opal. A solution of titanium ethoxide and dry ethanol was produced, to which the dried latex spheres (*ca.* 1% vol) were added. The mixture was agitated in an ultrasonic bath and then poured into a small vial in which a quartz plate had been placed. The vial was positioned in a vibration-free, temperature-controlled environment for about a week, until all of the liquid had evaporated. On removal, the slide, now coated with a white deposit on both sides, was placed in the tube furnace and calcined at 575 °C. SEM investigation of the initial products revealed the presence of some latex spheres that had not been removed during calcination. These spheres were successfully removed by calcining the sample at a slightly higher temperature (650 °C). The samples obtained did show ordered arrays of air spheres but the film had broken up into microcrystallites approximately 2 μm in size (Fig. 3d). It seems likely that this effect is associated with the lattice strain that builds up in the crystal during calcination and is consistant with previous observations.[10,28] SEM measurements show that the distance between the centres of the air spheres is 15–20% smaller than diameter of the latex spheres used. This shrinkage during calcination will result in a substantial isotropic compressive stress on the crystal. In the absence of a substrate (*i.e.* the first approach used) the crystal appears to accommodate this stress. In the capillary experiments the presence of significant attractive forces between the thin film and the substrate, evidenced by the higher calcination temperature required, appears to cause the break-up of the polycrystalline film into individual microcrystallites.

In summary, we have described three routes for the synthesis of inverse opal based on titania. While all of the methods produce well-ordered photonic crystals, the mechanical strength of the product depends on the method of preparation used. The simple filtration method produces large robust platelets of inverse opal that are ideally suited for investigation of the photonic properties of this exciting new material.

6 Optical properties of opal and inverse opal

Optical reflectance is the most direct way to measure the photonic stopband behaviour. Compared with transmission methods, minimal specimen preparation is necessary and the effective refractive index and inter-planar spacing can be determined.[26] Optical reflectance measurements were performed using a white light source and monochromator, with equal angles of incidence and reflection, together with a germanium detector, or a photomultiplier tube, and lock-in amplifier. The resulting spectra from opal formed using 545 nm

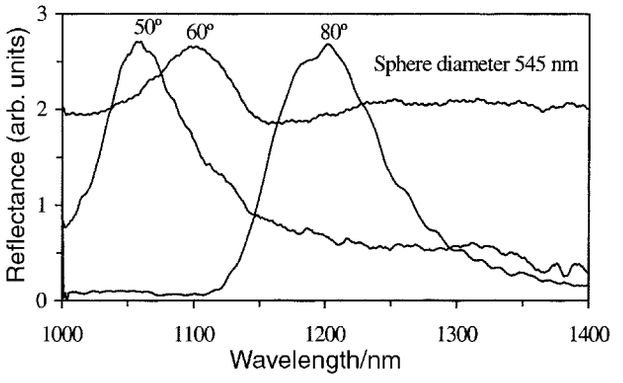

Fig. 4 Reflectance spectra of normal opal at various angles of incidence.

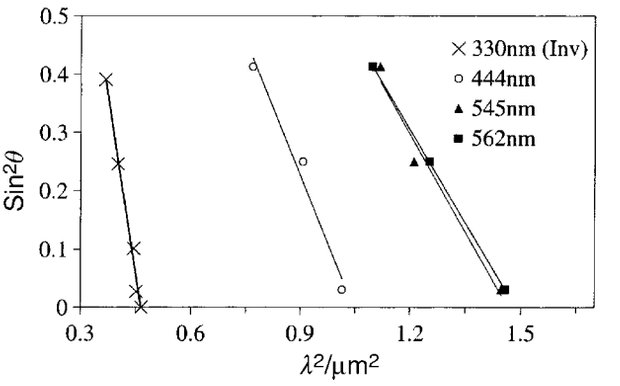

Fig. 5 Plot of square of the free-space wavelength of light (reflection maxima) versus $\sin^2\theta$, where θ is the angle of incidence to the surface normal.

diameter silica spheres are shown in Fig. 4 for different angles of incidence measured with respect to the surface.

Bragg's law and Snell's law can be combined to describe the position of the angle resolved reflection peaks.[29,30] The modified form of Bragg's law, which takes into account the reduced angle with respect to the normal at which light travels in the opal (*i.e.* taking into account Snell's law), can be written as,

$$\lambda = 2d(n_{\text{eff}}^2 - \sin^2\theta)^{1/2} \quad (1)$$

where λ is the free-space wavelength of light, d is the inter-planar spacing, n_{eff} is the effective refractive index and θ is the angle measured from the normal to the planes. It has been shown that the calculated effective refractive index, based on the volume fraction of the respective dielectric components, correlates well with the filling fraction.[31] The inter-planar spacing, d, can be expressed in terms of the unit cell parameter a, and the Miller indices: $d = a/(h^2+k^2+l^2)^{1/2}$. For the fcc lattice, the diameter of the spheres D is related to the lattice parameter by $a = \sqrt{2}D$. Assuming that the reflection occurs from the (111) planes (the most densely packed), a plot of λ^2 *versus* $\sin^2\theta$ yields n_{eff} and d, from which D can be calculated (Fig. 5). The results of these calculations are tabulated in Table 2, where they are compared with sphere size measurements (SEM) and literature results.

Fig. 6 shows the reflectance spectra measured at different angles of incidence on titania inverse opal. The asymmetric peaks are much wider than the peaks typical of good quality opal[29] and are consistent with the results published by other workers.[33] At normal incidence, the ratio of the width at half height (ΔE) to the position of the reflectance peak (E_c) gives a normalised measure of the photonic stopband. For the titania matrix, this ratio is 0.15, which is approximately twice the value for normal opal, *ca.* 0.07. Following the procedure above and assuming that the reflection peaks observed are associated with

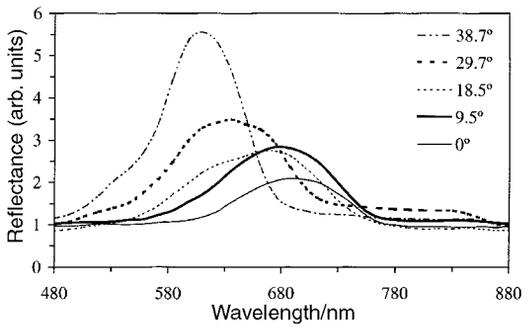

Fig. 6 Reflectance spectra of inverse opal at various angles of incidence.

Table 2 Comparison of sphere sizes obtained from SEM measurements with those calculated from reflectivity measurements. Also shown are the values for the effective refractive index (n_{eff}) and normalised photonic stopband ($\Delta E/E_c$) obtained from optical measurements

	Inverse opal		Opal				
Source	This work	Ref. 10	This work			Ref. 30	Ref. 32
Measured sphere diameter/nm	330	395	444	545	562	236	380
Calculated sphere diameter/nm	306		493	573	594		
n_{eff}	1.37		1.27	1.28	1.26	1.39	
$\Delta E/E_c$	0.15	0.10	0.07	0.08	0.08	0.06	0.07

the (111) planes of a fcc lattice of air spheres, we obtain, from Fig. 6, a centre-to-centre separation of 306 nm. This value is in good agreement with the value of 330 nm measured from the SEM images (Table 2).

The calculated and measured values of sphere diameter in normal opal agree within 11, 5 and 6% respectively. Although the opal produced in the current project has somewhat larger spheres than in the work by Romanov *et al.*[30] (236 nm), the estimated effective refractive index is lower (1.27 compared to 1.39) and is similar to that found by other workers.[32] In both ref. 30 and 32, the materials appear to have undergone more extensive sintering. The titania inverse opal structure is mechanically weak, but possesses a relatively large bandgap of $\Delta E/E_c = 0.15$. This result is in contrast with that for the material described by Subramania *et al.*,[10] which possesses a bandgap of approximately two thirds this value. However, their structure had been compressed along the [111] direction to reduce crack formation. In general, sintering of normal opal can increase its mechanical strength and its effective refractive index. Similar improvements in inverse opal can be achieved by compression. However, this improvement in mechanical properties is at the expense of reducing the PBG in the [111] direction.[19]

In summary, using optical reflectance, we have demonstrated that the normal and inverse opal samples produced in this work exhibit a photonic stopband. The agreement between the sphere size measured by microscopy techniques and that calculated from the optical reflectance measurements is encouraging, as it suggests that the materials produced exhibit photonic crystal behaviour over a large area of the sample.

7 Conclusions

High quality synthetic opal photonic crystals can be formed by controlled self-organisation of colloidal silica spheres. In this paper, we have demonstrated that control of both sphere size and "deposition" conditions is required if total synthesis is to be achieved. Varying the ammonia concentration in the reaction mixture can be used to control the sphere size, but the size of the product can vary by around 3% even when the same nominal composition is used. We have demonstrated that the way in which the mother liquors are combined to produce the reaction mixture has a significant impact on the sphere size and is the likely origin of the discrepancy in sphere size. We have also demonstrated that large well-ordered crystals of synthetic opal that exhibit a photonic stopband can be produced in less than 24 h using an ultracentrifuge to aid sedimentation. Thin films of well-ordered opal that exhibit opalescence have been formed using the capillary method and this approach shows great promise for the formation of opal on technologically important substrates.

The novel microporous material known as inverse opal has great potential as a photonic crystal, as the topology of this material results in an inherently larger bandgap than normal opal. Our results suggest that the bulk methods for production of these structures are likely to be more successful than thin film techniques. In the thin film method, we believe that the lattice strain induced during calcination cannot be accommodated by the structure and results in the destruction of the continuous thin film. The photonic properties of the bulk crystals are excellent and inverse opal structures are likely to have a significant impact in the realisation of useful photonic crystals.

Acknowledgements

The authors would like to acknowledge the contributions of Jim Gallagher, Donald MacLaren, Graham Noble, Arnaud Richel and Rebecca Thomson to the development of the experimental methods used in this project. We are grateful to the EPSRC (GR/M16542) and DERA for financial support.

References

1 E. Yablonovitch, *Phys. Rev. Lett.*, 1987, **58**, 2059.
2 S. John, *Phys. Rev. Lett.*, 1987, **58**, 2486.
3 T. F. Krauss and R. M. De La Rue, *Prog. Quantum Opt.*, 1999, **23**, 51.
4 E. Yablonovitch, *J. Opt. Soc. Am. B*, 1993, **10**, 283.
5 J. V. Sanders and P. J. Darragh, *Mineral. Rec.*, 1971, **2**, 261.
6 M. E. Zoorob, M. D. B. Charlton, G. J. Parker, J. J. Baumberg and M. C. Netti, *Nature*, 2000, **404**, 740.
7 S. G. Romanov, N. P. Johnson, A. V. Fokin, V. Y. Butko, H. M. Yates, M. E. Pemble and C. M. S. Torres, *Appl. Phys. Lett.*, 1997, **70**, 2091.
8 B. T. Holland, C. F. Blanford and A. Stein, *Science*, 1998, **281**, 538.
9 B. T. Holland, C. F. Blanford, T. Do and A. Stein, *Chem. Mater.*, 1999, **11**, 795.
10 G. Subramania, K. Constant, R. Biswas, M. M. Sigalas and K.-M. Ho, *Appl. Phys. Lett.*, 1999, **74**, 3933.
11 J. E. G. J. Wijnhoven and W. L. Vos, *Science*, 1998, **281**, 802.
12 A. Blanco, E. Chomski, S. Grabtchak, M. Ibisate, S. John, S. W. Leonard, C. Lopez, F. Meseguer, H. Miguez, J. P. Mondia, G. A. Ozin, O. Toader and H. M. van Driel, *Nature*, 2000, **405**, 437.
13 W. Stober, A. Fink and E. Bohn, *J. Colloid Interface Sci.*, 1968, **26**, 62.
14 P. Jiang, J. F. Bertone, K. S. Hwang and V. L. Colvin, *Chem. Mater.*, 1999, **11**, 2132.
15 A. K. Van Helden, J. W. Jansen and A. Vrij, *J. Colloid Interface Sci.*, 1981, **81**, 354.
16 S. Chen, P. Dong, G. Yang and J. Yang, *J. Colloid Interface Sci.*, 1996, **180**, 237.
17 C. G. Tan, B. D. Bowen and N. Epstein, *J. Colloid Interface Sci.*, 1987, **118**, 290.
18 A. Van Blaaderen, J. Van Geest and A. Vrij, *J. Colloid Interface Sci.*, 1992, **154**, 481.
19 K. Busch and S. John, *Phys. Rev. E.*, 1998, **58**, 3896.
20 L. V. Woodcock, *Nature*, 1997, **385**, 141; L. V. Woodcock, *Nature*, 1997, **388**, 235.
21 P. N. Pusey, W. van Megen, P. Bartlett, B. J. Ackerson, J. G. Rarity and S. M. Underwood, *Phys. Rev. Lett.*, 1989, **63**, 2753.
22 H. Miguez, F. Meseguer, C. Lopez, A. Mifsud, J. S. Moya and L. Vazquez, *Langmuir*, 1997, **13**, 6009.
23 L. N. Donselaar, A. P. Philipse and J. Suurmond, *Langmuir*, 1997, **13**, 6018.
24 M. Dongbin, L. Hongguang, C. Bingying, L. Zhaolin, Z. Daozhong and D. Peng, *Phys. Rev. B*, 1998, **58**, 35.
25 S. Tsunekawa, Y. A. Barnakov, V. V. Poborchii, S. M. Samoilovich, A. Kasuya and Y. Nishina, *Microporous Mater.*, 1997, **8**, 275.
26 R. Mayoral, J. Requena, J. S. Moya, C. Lopez, A. Cintas,

H. Miguez, F. Meseguer, L. Vazquez, M. Holgado and A. Blanco, *Adv. Mater.*, 1997, **9**, 257.
27 A. Richel, N. P. Johnson and D. W. McComb, *Appl. Phys. Lett.*, 2000, **76**, 1816.
28 G. Subramania, K. Constant, R. Biswas, M. M. Sigalas and K.-M. Ho, *J. Lightwave Technol.*, 1999, **17**, 1970.
29 C. Lopez, L. Vazquez, F. Meseguer, R. Mayoral, M. Ocana and H. Miguez, *Superlattices Microstruct.*, 1997, **22**, 399.
30 S. G. Romanov, A. V. Fokin and R. M. De La Rue, *J. Phys.: Condens. Matter*, 1999, **11**, 3593.
31 S. G. Romanov, A. V. Fokin, H. M. Yates, M. E. Pemble, N. P. Johnson and R. M. De La Rue, *IEE Proc. Optoelectron.*, 2000, **147**, 138.
32 H. Miguez, A. Blanco, C. Lopez, F. Meseguer, H. M. Yates, M. E. Pemble, F. Lopex-Tejeira, F. J. Garcia-Vidal and J. Sanchez-Dehesa, *J. Lightwave Technol.*, 1999, **17**, 1975.
33 M. S. Thijssen, R. Sprik, J. E. G. J. Wijnhoven, M. Megens, T. Narayanan, A. Lagendijk and W. L. Vos, *Phys. Rev. Lett*, 1999, **83**, 2730.